Hindawi
Journal of Analytical Methods in Chemistry
Volume 2019, Article ID 7590692, 9 pages
https://doi.org/10.1155/2019/7590692

Research Article

Study on Blending of Wall Material of the Nonel Tube by CSW/PE-g-MAH

Hong-wei Li,[1] Bin-bin Zhang,[1] Ji-nian Yang ,[2] Huan Li,[1] Ji-chang Gui ,[1] and Zhan Lei[1]

[1]*School of Chemistry and Chemical Engineering, Anhui University of Science and Technology, Huainan 232001, Anhui, China*
[2]*School of Material Science and Engineering, Anhui University of Science and Technology, Huainan 232001, Anhui, China*

Correspondence should be addressed to Ji-nian Yang; 33249596@qq.com

Received 6 May 2019; Accepted 18 November 2019; Published 23 December 2019

Academic Editor: Luca Tortora

In order to improve the strength and resistance of ordinary nonel tubes, calcium sulfate whiskers (CSW, treated with silane coupling agent) and maleic anhydride grafted polyethylene (PE-g-MAH) are used to control the wall material of the nonel tube that the blending of the low-density polyethylene was enhanced. The effects of mass fraction of CSW or PE-g-MAH on the tensile properties, interfacial structure, melting and crystallization characteristics, and thermal decomposition behavior of the composite system were studied, and the thermal decomposition kinetics were calculated. The results show that, relative to pure LDPE, the strength of LDPE/CSW (85/15) is increased by 7.58%, and the strength of LDPE/CSW/PE-g-MAH (84/15/1) is increased by 7.58%. The addition of CSW or PE-g-MAH has gradually changed the fracture mode of the LDPE matrix. Thermal analysis shows that CSW can reduce the crystallinity of LDPE. The melting and crystallization characteristics of LDPE/CSW/PE-g-MAH composites have little effect, but the thermal decomposition stability is improved. The kinetic analysis showed that the reaction order (n) was around 1, CSW could improve LDPE/CSW thermal decomposition activation energy, and PE-g-MAH increased the thermal decomposition activation energy of LDPE/CSW/PE-g-MAH.

1. Introduction

Ordinary nonel tube has excellent ignition characteristics. The whole blasting network can be triggered by electric spark, which avoids the requirement of electric network for initiating current [1, 2]. The detonation method of the nonel tube was observed under high-speed cameras [3, 4], and the design and connection method of the blasting network was widely studied and applied [5–8]. The source material of ordinary plastic nonel tube is low-density polyethylene (LDPE), which has the characteristics of good toughness, easy processing, and wide application range [9–13]. With the development of the civil explosive industry, the use of the existing ordinary nonel tube is limited, and new requirements are imposed on the strength and heat resistance of the nonel tube.

For decades, people's research on detonating tubes has focused on the study of high-intensity and high-precision and supporting detonators. The core of the research was the delay accuracy of nonel tubes [14–16]. There was also research on the color-changing nonel tube to explore the discoloration performance of elements such as aluminum and chlorine in the nonel tube [17, 18]. The purpose of these studies was to improve the strength and heat resistance of the nonel tube and to increase the range of use of the nonel tube. In view of this, this paper intends to use the basic research on the material of the nonel tube to explore the blending modification of LDPE, to prepare a low-cost high-strength low-density polyethylene nonel tube, and to improve the scope of use of plastic nonel tube.

Calcium sulfate whiskers (CSW) were artificial crystals, which were commonly used to modify the strength of composites [19–23]. For example, in the study of the mechanical properties of CW-enhanced modification, the modified CSW has a strong interfacial bond with the PVC matrix [22], and CSW could effectively improve the thermal stability of the material [23]. Maleic anhydride grafted polyethylene (PE-g-MAH) is a compatibilizer commonly

used to increase the compatibility of the infused system and improve the physical and chemical properties of the matrix [24–28]. For example, PE-g-MAH not only improved the thermal stability of LDPE/ESP composites, but also improved its interfacial bonding [26]. The addition of PE-g-MAH also improved tensile strength and Young's modulus of the LDPE/NR/WHF composites [27]. However, there are few reports on the blending of LDPE/CSW/PE-g-MAH. In this paper, based on the strength of CSW-enhanced LDPE, the strength is increased again by adding the compatibilizer PE-g-MAH. By observing the cross-sectional morphology and melt crystallization properties of LDPE/CSW/PE-g-MAH composites and analyzing their thermogravimetric losses, the apparent activation energy was calculated and compared by Kissinger [29] and Carrasco et al. [30, 31], who provided a reference for obtaining a material with high strength and good heat resistance.

2. Experimental

2.1. Raw Materials. LDPE (1I2A-1, China Petrochemical Co., Ltd. Beijing Yanshan Branch, China) is a pellet with a density of 0.92 g/cm^3 and a melt flow rate (MFR) of 2.0 g/10 min. Powders of CSW (white, Tang Brothers Technology Co., Ltd, Wuhan, China) have a density of 2.69 g/cm^3 and a length-to-diameter ratio of 30 to 70, which is a crystal form of calcium sulfate hemihydrate $CaSO4{\cdot}0.5H_2O$. Silane coupling agent, KH550, Nanjing Dawn Chemical Co., Ltd., analysis pure. The compatibilizer PE-g-MAH (manufactured by Dow, USA) is a pellet with a melt flow rate (MFR) of 2.5 g/10 min and a density of 0.95 g/cm^3. Reagents such as anhydrous ethanol, silicone oil, and liquid paraffin are of analytical grade and are commercially available.

2.2. Preparation of Samples. According to the literature [32], in order to improve the interface compatibility between CSW and LDPE, the surface modification of CSW with KH550 was carried out.

An appropriate amount of LDPE, CSW, and PE-g-MAH was weighed and dried under vacuum at 60°C for 24 hours. A high-speed mixer (SHR-10A, Zhangjiagang Jianguo Machinery Co., Ltd) is used for premixing according to the ratio shown in Table 1 and is subjected to melt extrusion through a double-screw extruder (SHJ-20, Nanjing Jaya Co., Ltd), and water-cooled granulation, and the temperature of I ~ VI temperature zones was 185°C, 190°C, 195°C, 190°C, 195°C, and 185°C, and the cooling water temperature was 17°C. The new material was again vacuum-dried at 60°C for 24 h and then injection molded (170–200°C) into a strip in a vertical injection molding machine (FT-200, Fomtec Machinery Co., LTD, Suzhou, China) (GB/T 1040.2-2006, 1A), standard dumbbell type.

2.3. Measurements

2.3.1. Mechanical Tests. Each sample was measured prior to the uniaxial tensile test. The span length test of the standard dumbbell type test was 62 mm, the length was 80 mm, the width was 10 mm, and the thickness was 4 mm. The uniaxial tensile test was carried out according to the Chinese Standard GB/T 1040.1-2006 on a universal electronic testing machine (WDW-50, Shenzhen Kaiqiangli Co., LTD, China) at a rate of 50 mm/min. The gauge length (type 1A) of the dumbbell-shaped specimen was 50 mm, and the impact test was performed on a TCL-25J impact tester (Tanhor Co., LTD, Jilin, China). The impact test results directly give the impact energy of each sample. The elastic modulus, elongation at break, tensile strength, and other values of the sample are obtained by an auxiliary computer, and the strain-stress curve is integrated to obtain the tensile toughness. All test results are taken from the average of 5 sets of samples and are carried out at room temperature.

Table 1: Mass fraction ratio of LDPE/CSW/PE-g-MAH composites.

Sample	LDPE (%)	CSW (%)	PE-g-MAH (%)
100/0/0	100	—	—
85/15/0	85	15	—
84/15/1	84	15	1
82/15/3	82	15	3
80/15/5	80	15	5
78/15/7	78	15	7
76/15/9	76	15	9

2.3.2. Scanning Electron Microscopy (SEM). A sample with higher quality was selected, and the sample was transferred to a bucket containing liquid nitrogen using a wooden stick and frozen for 20 minutes. The sample was taken out and the brittle fracture treatment was carried out using the brittle cutting machine, the sample was collected, the section should not be touched by hand, and $4 * 4$ mm small pieces were taken at the section. The brittle fracture section was subjected to Au spray treatment, and then the cross-sectional morphology was observed by field emission scanning electron microscopy (FESEM, JSM 7600F, JEOL Ltd., Japan).

2.3.3. Differential Scanning Calorimeter (DSC). Non-isothermal melting and cooling curves of the samples were obtained using a differential scanning calorimeter (DSC, Q200, TA, USA). The temperature rise and fall rate of the DSC was 10°C/min, and the reaction was carried out under an N_2 atmosphere at a concentration of 60 mL/min. The temperature was raised from room temperature to 180°C for 10 min and then lowered to room temperature.

2.3.4. Thermogravimetric Analysis (TGA). The mass loss and mass loss rate curves were obtained using a thermogravimetric analyzer (TGA, Q500, TA, USA) and the temperature was raised from room temperature to 700°C. The amount of sample in the alumina crucible was about 15 mg, in an N_2 atmosphere at a flow rate of 60 mL/min, and the temperature was raised at a rate of 10°C/min.

3. Results and Analysis

3.1. Mechanical Properties. The stress-strain curves of LDPE/CSW/PE-g-MAH composites are shown in Figure 1, and other mechanical properties are shown in Table 2. The tensile strength, elastic modulus, and elongation at break of the material correspond to their strength, stiffness, and toughness [33–35]. Figure 1 shows that, after adding CSW, the strength and stiffness are improved. After adding PE-g-MAH, the strength and stiffness are increased again, but as the mass fraction of PE-g-MAH increases, the increase in the tensile strength and modulus of elasticity of the composite material was less. The introduction of CSW showed that the matrix fracture failure mode of LDPE changed, and the reintroduction of PE-g-MAH increased the compatible phase of LDPE/CSW interface and strengthened the fracture failure mode of 85/15/0. The tensile toughness calculated according to the method of [36] is shown in Table 2 and is substantially consistent with its toughness and is reduced. The addition of PE-g-MAH increased the tensile strength and Young's modulus of LDPE/NR/WHF composites, and the tendency of elongation at break was consistent [27].

The stiffness of LDPE/CSW/PE-g-MAH composites increased by 75.93%~93.79%, that is, the resistance to elastic deformation was enhanced effectively, ensuring that the nonel tube is not subjected to artificial pressure to cause the powder to fall off and gather. After adding 15% CSW to LDPE, the 85/15/0 strength increased by 7.58% (0.91 MPa), with the addition of PE-g-MAH with mass fraction of 1%, 3%, 5%, 7%, and 9%, the strength increased by 18.90%~23.14% (2.27~2.78 MPa), and the strength increased significantly. It is not difficult to find that by adding only 1% PE-g-MAH, the 84/15/1 strength can be increased by 19.98% (2.4 MPa), and for the preparation of the nonel tube, the heat resistance and production cost of the material should also be considered, but the addition amount of PE-g-MAH should not exceed 5%.

3.2. Microstructure. Figure 2 shows an SEM image of the impact profile of LDPE/CSW/PE-g-MAH composites after cryogenic brittle fracture of liquid nitrogen. It can be seen from the visible whiskers and the pores left after the detachment that the CSW or PE-g-MAH is evenly distributed in the cross section of the sample, and no obvious agglomeration occurs. Under high magnification, the 85/15/0 composite material and the 84/15/1 and 80/15/5 composite materials have obvious differences in cross section. The interface between the CSW and the LDPE matrix was very tight, and the exposed whisker surface was covered with a layer of resin adhering matter, and the pores scattered around it showed obvious irregularities. Figure 2(b) shows that the fracture process of the material is not completely in the matrix, and there is a large area of exposed whisker interface, and it is proved that the process of breaking the CSW and LDPE has the dissociation of the interface between CSW and LDPE in addition to the tear of the matrix; it is consistent with the increase in 85/15/0 strength in the mechanical properties, as shown in Table 2. The addition of

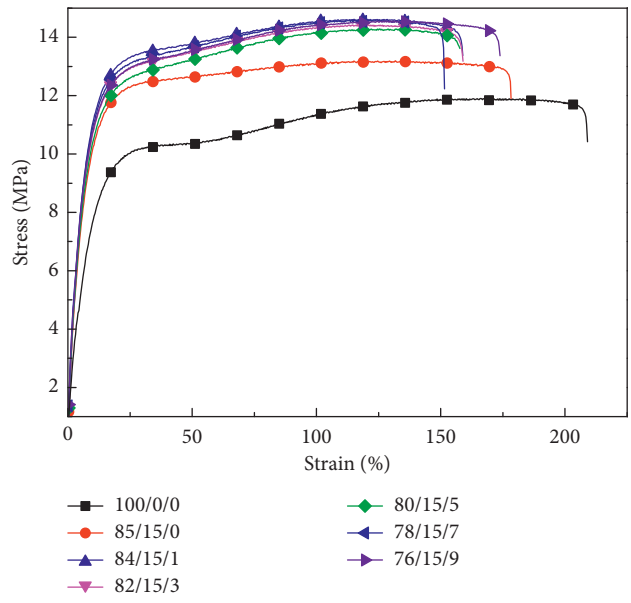

Figure 1: Stress-strain curve of LDPE/CSW/PE-g-MAH composites.

1% PE-g-MAH, such as the existence of (d) diagram compatibilizer PE-g-MAH, will reduce the exposed whisker interface in the cross section. Combined with the strength and stiffness properties of 84/15/1 in Figure 1 and Table 2, the dissociation is weak at this time, and the matrix tear is the main failure mode of the composite; it is consistent with the conclusion that PE-g-MAH can change the interface bonding property of composites in [26]. As shown in Figure 2(f), the whiskers of the 80/15/5 section are tightly covered by the LDPE resin adherend, and the fracture process has substantially no interface dissociation, which is completely the matrix tear. The main reason for this is that in addition to the organic functionalization of the surface of the CSW by the interface coupling agent, it has good interfacial compatibility with the LDPE matrix, and it also benefits from the compatibilization of PE-g-MAH, which makes the compatibility of the interface between CSW and LDPE complete, which is very beneficial to improve the mechanical properties of the composite.

3.3. Melting and Crystallization. Through the characterization of mechanical properties and cross section morphology, the LDPE/CSW/PE-g-MAH ratio component with improved strength is obtained. However, as an important material for detonating tube wall, heat resistance is also an important standard in addition to strength, which is also an important standard. Figure 3 shows the DSC heating curve of LDPE/CSW/PE-g-MAH composites. According to the melt-crystallization enthalpy (ΔH_m) of 23.75 J/g, when LDPE is completely crystallized [36], the crystallinity (X_c) of the composite material and the melting temperature peak temperature (T_m) of LDPE can be calculated and are shown in Table 3. The T_m of 85/15/0 has decreased, and on the basis of it, 84/15/1 and 80/15/5 have been improved, but the T_m range of all samples is 113.06~113.88°C, and the fluctuation

Table 2: Mechanical properties of LDPE/CSW/PE-g-MAH composites.

Sample	Tensile strength (MPa)	Elastic modulus (MPa)	Elongation at break (%)	Tensile toughness (MJ/m^3)
100/0/0	12.01	103.57	203.04	22.64
85/15/0	12.92	158.98	167.53	22.24
84/15/1	14.41	182.21	150.92	21.64
82/15/3	14.43	191.20	152.30	21.25
80/15/5	14.28	180.55	158.83	21.09
78/15/7	14.61	200.14	149.84	20.46
76/15/9	14.79	199.62	175.20	21.54

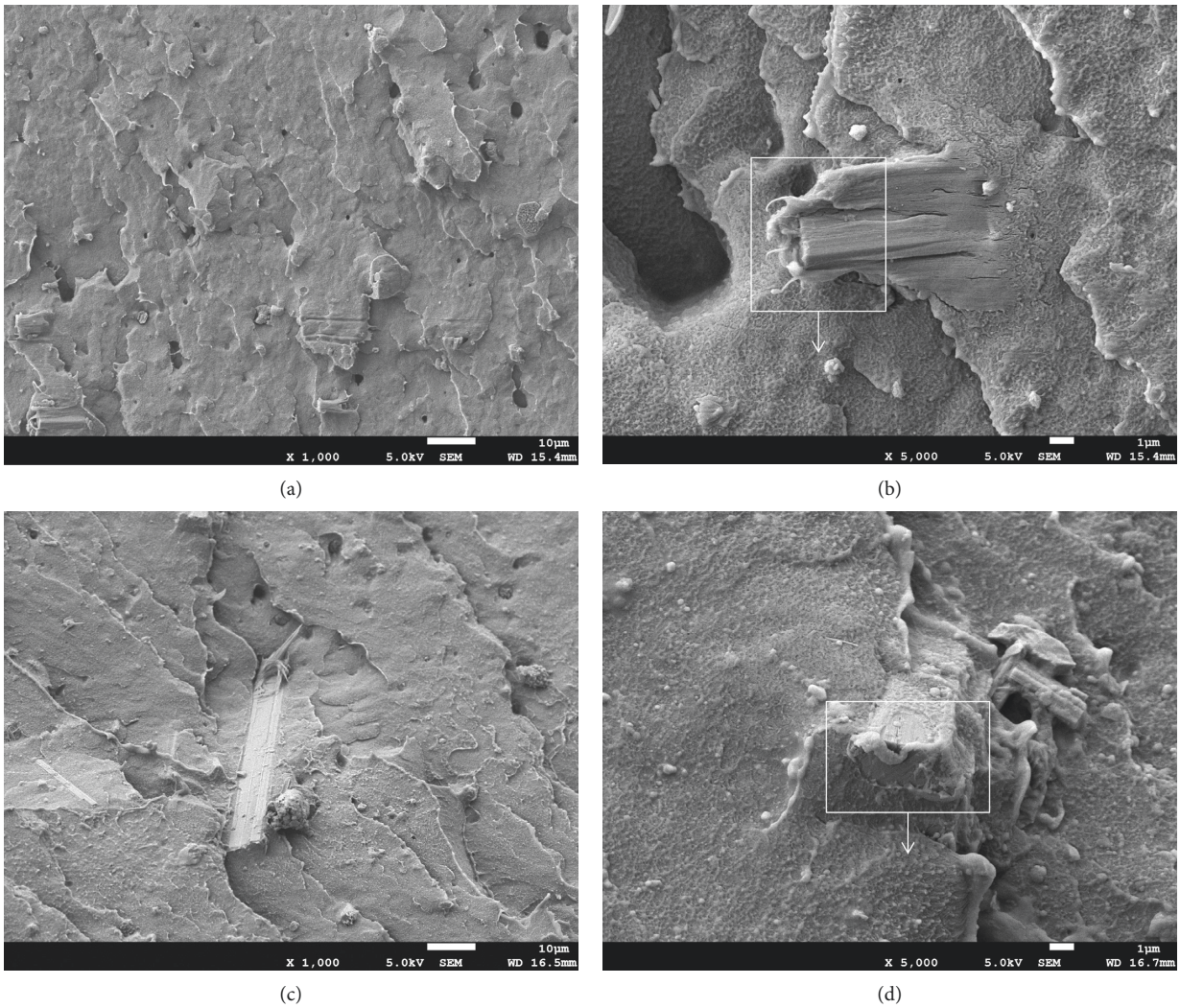

(a) (b)

(c) (d)

Figure 2: Continued.

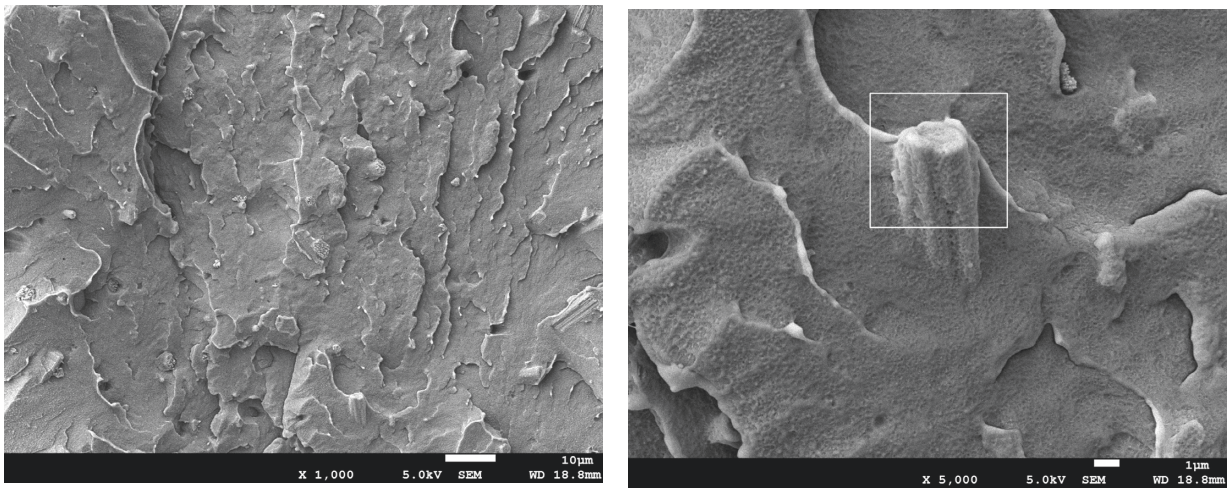

(e) (f)

Figure 2: Microstructures of LDPE/CSW/PE-g-MAH composites: (a)~(b) 85/15/0, (c)~(d) 84/15/1, and (e)~(f) 80/15/5.

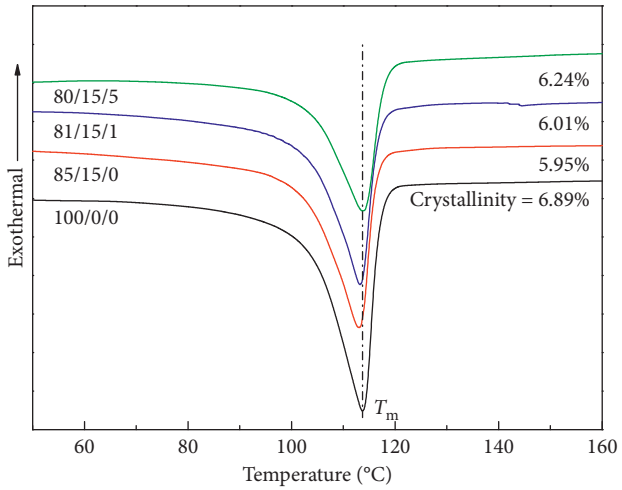

Figure 3: DSC heating curve of LDPE/CSW/PE-g-MAH composites.

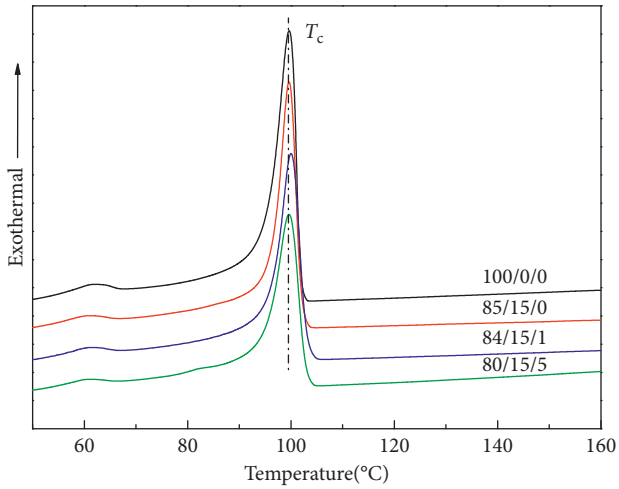

Figure 4: DSC cooling curve of LDPE/CSW/PE-g-MAH composites.

Table 3: Melting and crystallization parameters of DSC curves of LDPE/CSW/PE-g-MAH composites.

Samples	T_c (°C)	T_m (°C)	ΔH_m (J/g)	X_c (%)
100/0/0	99.66	113.68	15.65	3.89
85/15/0	99.06	113.06	13.52	5.95
84/15/1	100.02	113.27	13.64	6.01
80/15/5	99.56	113.88	14.16	6.24

ΔH_m is corrected for the percentage of LDPE phase in the composites.

range is small. It indicates that the introduction of CSW or PE-g-MAH has little effect on the T_m of LDPE/CSW/PE-g-MAH composites.

Figure 4 shows the DSC cooling curve of the LDPE/CSW/PE-g-MAH composite material, and the crystallization peak temperature (T_c) is shown in Table 3. The temperature of T_c is between 99.06 and 100.2°C, and the fluctuation range is also small, which has little effect on it. The trend of crystallinity was consistent with T_m. The combination may be that PE-g-MAH hindered the blocking effect of CSW on crystallization of LDPE, and the overall crystallinity of LDPE/CSW/PE-g-MAH increased. In general, from the melting and crystallization properties of LDPE/CSW/PE-g-MAH composites, either CSW or PE-g-MAH has little effect on LDPE. However, there are no restrictions on the melting and crystallization properties of LDPE.

3.4. Thermal Decomposition Characteristics. Figure 5 shows the TG curve of LDPE/CSW/PE-g-MAH composite, and the initial weight loss temperature (T_o) (5% weight loss of TG), 600°C weight loss residual mass fraction (W_{600}), and final weight loss residual (Char (%))are shown in Table 4. CSW or PE-g-MAH had a constant weight in weight loss at 600°C

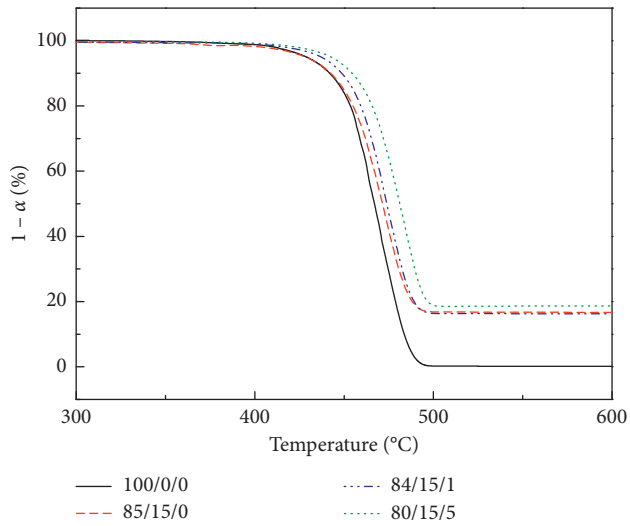

Figure 5: TG curve of LDPE/CSW/PE-g-MAH composites.

Table 4: Thermal degradation parameters for LDPE/CSW/PE-g-MAH composites.

Sample	T_o (°C)	T_p (°C)	α_p (%)	$(d\alpha/dT)_p$ (% (°C))	W_{600} (%)	Char (%)
100/0/0	428.92	470.34	58.66	2.616	0.17	0.03
85/15/0	428.25	473.33	54.35	2.253	16.69	16.57
84/15/1	437.08	472.98	47.73	2.453	16.27	16.21
80/15/5	442.73	483.43	55.45	2.421	18.67	18.51

and higher because $CaSO_4{\cdot}0.5H_2O$ in CSW decomposes $CaSO_4$ at high temperature. In addition, T_o of the 85/15/0 was lowered by 0.67°C with respect to 100/0/0 because the H_2O molecules of $CaSO_4{\cdot}0.5H_2O$ in CSW were decomposed in the low-temperature region. T_o of 85/15/0 and 80/15/5, respectively, moved 8.16°C and 13.81°C to the high-temperature zone. This is because the weight loss temperature of CSW or PE-g-MAH is higher than that of LDPE, which improves LDPE/CSW/PE-g-MAH composite heat resistance.

Figure 6 shows the DTG curve of the LDPE/CSW/PE-g-MAH composite. The maximum decomposition temperature T_p, the conversion rate α_p (%), and the maximum decomposition rate $(d\alpha/dT)_p$ (%/K) are shown in Table 4. The addition of CSW or PE-g-MAH shifted the T_p of DTG of LDPE/CSW/PE-g-MAH composites to 2.64~13.09°C in the high-temperature region and decreased $(d\alpha/dT)_p$ by 0.163–0.363%/K. α_p decreased by 3.21~10.93%, and the fluctuation was significant, indicating that the thermal decomposition stability of LDPE/CSW/PE-g-MAH composites was improved. Considering the economic cost of enhanced modification, combined with the mechanical properties of 84/15/1, the amount of PE-g-MAH should be higher than 1%, but not 5%, because the cost of 80/15/5 will increase a lot. Because the cost of 80/15/5 will increase a lot, considering its mechanical and thermal properties, it is not as good as 84/15/1.

3.5. Thermal Decomposition Kinetics Calculation. Figure 7 shows the first derivative curve of the mass loss rate of LDPE/CSW/PE-g-MAH composites, reflecting the trend

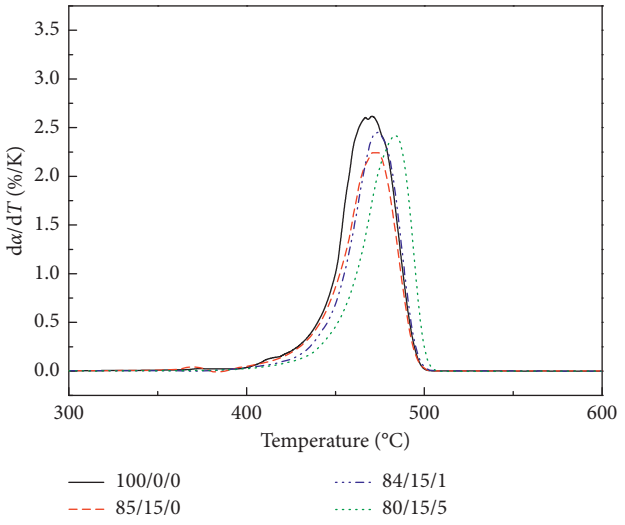

Figure 6: DTG curve of LDPE/CSW/PE-g-MAH composites.

of $d^2\alpha/dT^2$ with temperature (T). Theoretically, Kissinger [29] and Carrasco et al. [30, 31] first calculate the reaction order (n), and the apparent activation energy E (kJ/mol) of LDPE/CSW/PE-g-MAH composites was calculated according to the following equation:

$$E = nRT_p^2 \frac{(d\alpha/dT)_p}{(1-\alpha_p)}, \quad (1)$$

where R is the gas constant that is equal to 8.314 J/(mol K), $(d\alpha/dT)_p$ is the reaction rate at the temperature of T_p and

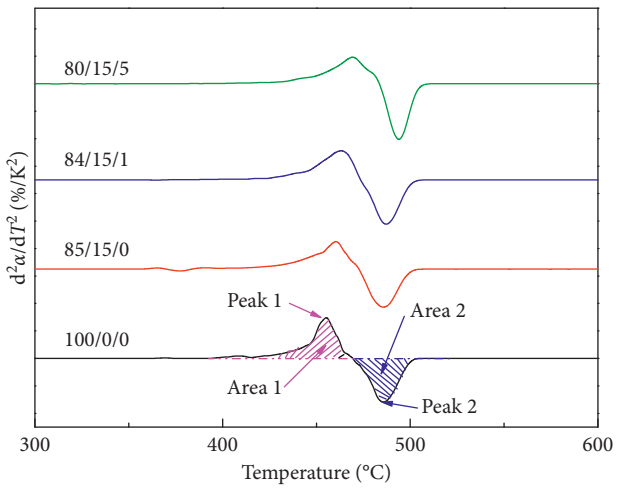

Figure 7: Variation of 2nd conversion derivative as a function of temperature for investigated samples.

from DTG curves, and α_p is the reaction conversion rate at the temperature of T_p and from TG curves.

The core of the calculation of the above two methods lies in the method of n. The Kissinger method mainly obtains S by the peak ratio, that is, S is equal to peak 1 and peak 2, S is a shape factor, and then n is calculated according to the following equation:

$$n = 1.26 \cdot \sqrt{S}. \tag{2}$$

Table 5: Reaction order (n) and activation energy (E) for LDPE/CSW/PE-g-MAH composites calculated by Kissinger and Carrasco methods.

Samples	Kissinger			Carrasco	
	s	n	E (KJ/mol)	n	E (KJ/mol)
100/0/0	0.752	1.092	317.66	0.917	266.68
85/15/0	0.662	1.025	234.37	0.941	215.16
84/15/1	0.765	1.102	239.37	1.041	226.12
80/15/5	0.573	0.954	246.95	0.921	238.41
		C. V = 0.0569		C. V = 0.0524	

However, the Carrasco method directly obtains n according to the ratio of the area, which is expressed in equation (2):

$$n = \frac{\int_{i_{(\alpha=0)}}^{T_p} \left(d^2\alpha/dT^2\right)_{\text{area 1}} \cdot dT}{\int_{p}^{T_{f(\alpha=\max)}} \left(d^2\alpha/dT^2\right)_{\text{area 2}} \cdot dT}, \tag{3}$$

where $(d^2\alpha/dT^2)$ is the rate of change of the reaction rate.

According to the detailed analysis of the literature, the calculation method of equation (4) is generally not used to obtain n [30, 31, 37] because n calculated by this method is a variation, so Kissinger and Carrasco are used, and the calculation of related parameters is performed. The results are shown in Table 5:

$$n = \frac{\ln\left[(d\alpha/dT)_p/(d\alpha/dT)\right]}{\left\{\left[T_p \cdot \left(T_p - T\right) \cdot (d\alpha/dT)_p\right]/\left[T \cdot \left(1-\alpha_p\right)\right]\right\} - \ln\left[(1-\alpha)/\left(1-\alpha_p\right)\right]}. \tag{4}$$

The range of n obtained by Kissinger is 0.954 to 1.092, and the range of n obtained by Carrasco is 0.917 to 1.041, and the overall difference is about 0.5, but the whole is also fluctuating around 1.00. The source of this error was related to the calculation method. S is only related to the peak value of the curve, but not related to the long or wide shape of the curve peak. That is to say, the use of S for n is lacking. The other reason is the error. It has been enlarged by 1.26 times and is usually better than the Carrasco method [37].

From Table 5, it is easy to find that the trend of n change obtained by the two methods of Kissinger and Carrasco is inconsistent, but the trend of the last calculated E is consistent. The addition of CSW will reduce the E of LDPE, which is consistent with the general rule of material blending. The inorganic material CSW usually reduces the E of the composite [37]. The addition of PE-g-MAH caused the E of LDPE/CSW to rise, but the increase of E was small. It may be that PE-g-MAH is caused by low molecular weight and small internal molecular chain. In combination with the Kissinger method, the E of 85/15/0 is 234.37 kJ/mol, the E of 84/15/1 is 239.37 kJ/mol, and the E of 80/15/5 is 246.95 kJ/mol. The span of E is small, but compared with the amount of PE-g-MAH added, it is also obvious. In addition, the span of E calculated by the Carrasco method is larger than that by the Kissinger method, but the E of 100/0/0 is 266.68 kJ/mol, which is less than the 317.66 kJ/mol (Kissinger method), and the coefficient of variation (CV) of the two methods is 0.0569 and 0.0524, respectively. The reason for the small difference is that there is a blending study of the three materials, and the properties of the composite material fluctuate greatly, but it still shows that the Carrasco method is more reliable.

In summary, the E reduction of LDPE/CSW/PE-g-MAH composites does not indicate a decrease in thermal decomposition stability. Because the E was calculated as T_p, the reaction progress α_p was less than 50%, and the thermal decomposition stability of the composite could not be directly judged. However, the addition of PE-g-MAH can increase E, which is beneficial to the E increase of LDPE/CSW/PE-g-MAH composites, and increases the thermal decomposition stability of the composite.

4. Conclusion

Through mechanical properties testing, adding 15% CSW to LDPE can increase its strength by 7.58%, the addition of a

small amount of compatibilizer increased the strength of the LDPE/CSW/PE-g-MAH composite, and the strength of 85/15/1 is 19.98% higher than that of pure LDPE. It has a positive significance for the strength increase of the nonel tube.

Through the observation under a high power microscope, it was found that the way of fracture changed. After adding 15% CSW to LDPE, the fracture mode was the coexistence of matrix tear and interface dissociation. With the addition of PE-g-MAH, the interface dissociation was limited. When the content of PE-g-MAH reaches 5%, the fracture mode of the interface is only the matrix fracture. It is well explained that the mechanical properties of LDPE/CSW/PE-g-MAH composites will be significantly improved in two stages.

The addition of CSW or PE-g-MAH has little effect on the melting and crystallization properties of the composite, but it has a certain improvement on the thermal decomposition stability and the T_o of 85/15/1 and 80/15/5 moved 8.16°C and 13.81°C, respectively, to the high-temperature zone. The addition of CSW or PE-g-MAH causes the T_p of the DTG of the LDPE/CSW/PE-g-MAH composite to move to the high temperature range of 2.64~13.09°C. $(d\alpha/dT)_p$ decreased by 0.163–0.363%/K, α_p decreased by 3.21~10.93%, and the fluctuation was significant, indicating that the thermal decomposition stability of LDPE/CSW/PE-g-MAH composites was improved. Through the two methods of Kissinger and Carrasco kinetic calculations, it is proved that PE-g-MAH can increase the E of the composite material, and the above conclusions are supported.

Data Availability

The data that are used to support the findings of this study are available from the first author upon reasonable request.

Conflicts of Interest

The authors declare that there are no conflicts of interest regarding the publication of this paper.

Acknowledgments

This article was supported by the Anhui Provincial Department of Education Major Scientific Research Project (KJ2019A0123) and National Natural Science Foundation of China (51404006).

References

[1] H. Fu, L. N. Y. Wong, Y. Zhao, Z. Shen, C. Zhang, and Y. Li, "Comparison of excavation damage zones resulting from blasting with nonel detonators and blasting with electronic detonators," *Rock Mechanics and Rock Engineering*, vol. 47, no. 2, pp. 809–816, 2014.

[2] D. B. Liu, D. Yang, R. G. Jiang et al., "Spectroscopic determination of the dynamic electrical spark temperature of nonel tube igniter," *Guang Pu Xue Yu Guang Pu Fen XI*, vol. 22, no. 4, pp. 670–672, 2002.

[3] Z. Sa-Sa, R. Gao-Feng, Sheng-Hai et al., "Research on the influence to detonation propagation reliability of broken hole nonel tube based on high-speed photography," *Engineering Blasting*, 2014.

[4] L. I. Ying, M. A. Guang-Ju, C. En-an et al., "Exploration of reliability of nonel tube firing in hole based on high-speed photography," *Blasting*, vol. 31, no. 4, pp. 129–133, 2014.

[5] L. Yang and P. Do, "Key parameters for controlling of function reliability in "NONEL" tube explosive transfer system," in *Proceedings of the Joint Propulsion Conference & Exhibit*, Los Angeles, CA, USA, June 1999.

[6] K. Kontis, *Shock Interactions with Structures and Their Associated Induced Flows*, pp. 157–170, Springer, Berlin, Germany, 2018.

[7] I. O. Samuelraj, G. Jagadeesh, and K. Kontis, "Micro-blast waves using detonation transmission tubing," *Shock Waves*, vol. 23, no. 4, pp. 307–316, 2013.

[8] J. Chen and L.-F. Xie, "Analysis of the factors influencing on the delay precision of nonel detonator," *Initiators & Pyrotechnics*, no. 6, pp. 21–24, 2012.

[9] A. Kumi-Larbi, D. Yunana, P. Kamsouloum, M. Webster, D. C. Wilson, and C. Cheeseman, "Recycling waste plastics in developing countries: use of low-density polyethylene water sachets to form plastic bonded sand blocks," *Waste Management*, vol. 80, pp. 112–118, 2018.

[10] L. Ge, W. Yang, H. Lv, M. Xia, X. Ji, and Z. Yao, "Colorating and mechanical performance of low-density polyethylene (LDPE)/dye-loaded shell powder (DPSP) composites (LDPE)/dye-loaded shell powder (DPSP) composites," *Fibers and Polymers*, vol. 16, no. 6, pp. 1294–1302, 2015.

[11] M. A. Tuasikal, O. Y. Alothman, M. Luqman, S. M. Al-Zahrani, and M. Jawaid, "Influence of natural and accelerated weathering on the mechanical properties of low-density polyethylene films," *International Journal of Polymer Analysis and Characterization*, vol. 19, no. 3, pp. 189–203, 2014.

[12] D. Fatih, K. Şirin, F. Kolcu, and İ. Kaya, "Conducting polymer composites based on ldpe doped with poly(aminonaphthol sulfonic acid," *Journal of Electrostatics*, vol. 94, pp. 85–93, 2018.

[13] V. Fombuena, D. García-Sanoguera, L. Sánchez-Nácher, R. Balart, and T. Boronat, "Optimization of atmospheric plasma treatment of ldpe films: influence on adhesive properties and ageing behavior," *Journal of Adhesion Science and Technology*, vol. 28, no. 1, pp. 97–113, 2014.

[14] Z. Jie, W. Zhang, J. Guo et al., "Application of high-strength and high-precision nonel detonator," *Explosive Materials*, 2005.

[15] D. Lin and P. Yang, "NONEL high precision MS delay detonator," *International Journal of Minerals Metallurgy and Materials*, vol. 8, pp. 164–166, 2001.

[16] C. Xia, J. Yang, D. Chen et al., "Comparative analysis of blasting vibration signal characteristics between high precision detonator and ordinary detonator," *Metal Mine*, 2011.

[17] Z. Bowen, Z. Shunguan, M. A. Xingyu et al., "Preparation and properties of a new kind of thermochromic plastic nonel," *Explosive Materials*, 2016.

[18] X. H. Cao and B. L. Yang, "Study on Cl color-changeable nonel tube," *Initiators & Pyrotechnics*, no. 1, pp. 7–10, 2001.

[19] Y. Wenjin, L. Yunhua, and X. Shiai, "Synthesis of a new titanate coupling agent for the modification of calcium sulfate whisker in poly(vinyl chloride) composite," *Materials*, vol. 9, p. 625, 2016.

[20] W. Yuan, J. Cui, Y. Cai et al., "A novel surface modification for calcium sulfate whisker used for reinforcement of poly(vinyl chloride)," *Journal of Polymer Research*, vol. 22, no. 9, p. 173, 2015.

[21] P. Ma, H. Chen, Q. Zhang, J. Wang, and L. Xiang, "Preparation of hierarchical caso4 whisker and its reinforcing effect on pvc composites," *Journal of Nanomaterials*, vol. 2018, pp. 1–7, 2018.

[22] J. Cui, Y. Cai, W. Yuan et al., "Preparation of a crosslinked chitosan coated calcium sulfate whisker and its reinforcement in polyvinyl chloride," *Journal of Materials Science & Technology*, vol. 32, pp. 745–752, 2016.

[23] J. N. Yang, S. B. Nie, and J. B. Zhu, "Fabrication and characterization of poly(lactic acid) biocomposites reinforced by calcium sulfate whisker," *Journal of Polymers and the Environment*, vol. 26, pp. 3458–3469, 2018.

[24] H. Zhai, W. Xu, H. Guo, Z. Zhou, S. Shen, and Q. Song, "Preparation and characterization of pe and pe-g-mah/montmorillonite nanocomposites," *European Polymer Journal*, vol. 40, no. 11, pp. 2539–2545, 2004.

[25] G. Liang, X. U. Junting, and X. U. Weibing, "Pe/pe-g-mah/org-mmt nanocomposites. II. nonisothermal crystallization kinetics," *Journal of Applied Polymer Science*, vol. 91, pp. 3054–3059, 2010.

[26] A. G. Supri, H. Ismail, and S. Shuhadah, "Effect of polyethylene-grafted maleic anhydride (PE-g-MAH) on properties of low density polyethylene/eggshell powder (LDPE/ESP) composites(pe-g-mah) on properties of low density polyethylene/eggshell powder (ldpe/esp) composites," *Polymer-Plastics Technology and Engineering*, vol. 49, no. 4, pp. 347–353, 2010.

[27] S. J. Tan, A. G. Supri, and P. L. Teh, "Effect of PE-g-MAH as compatibilizer on properties of LDPE/NR/WHF composites," *Applied Mechanics and Materials*, vol. 284–287, pp. 87–93, 2013.

[28] M. Z., S. H. Ahmad, A. Yarmo et al., "The effect of pe-g-mah plus γ-gps on shear strength of the aluminium/lldpe/aluminium (apea) laminate composite," *Advanced Materials Research*, vol. 576, pp. 276–279, 2012.

[29] H. E. Kissinger, "Reaction kinetics in differential thermal analysis," *Analytical Chemistry*, vol. 29, pp. 1702–1706, 1957.

[30] F. Carrasco, P. Pagès, J. Gámez-Pérez, and O. O. Santana, "Maspoch ML, kinetics of the thermal decomposition of processed poly(lactic acid)," *Polymer Degradation and Stability*, vol. 95, no. 12, pp. 2508–2514, 2010.

[31] F. Carrasco, J. Gamez-Perez, O. O. Santana et al., "Processing of poly(lactic acid)/organomontmorillonite nanocomposites: microstructure, thermal stability and kinetics of the thermal decomposition," *Chemical Engineering Journal*, vol. 178, pp. 451–460, 2011.

[32] D. LI, W. Y. TEOH, J. J. GOODING et al., "Functionalization strategies for protease immobilization on magnetic nanoparticles," *Advanced Functional Materials*, vol. 20, pp. 1767–1777, 2010.

[33] T. T. Mai, N. T. Chinh R. Baskaran et al., Tensile, thermal, dielectric and morphological properties of polyoxymethylene/silica nanocomposites," *Journal of Nanoscience and Nanotechnology*, vol. 18, no. 7, pp. 4963–4970, 2018.

[34] S. N. Monteiro, F. P. D. Lopes, and A. S. Ferreira, "Weibull analysis for the diameter dependence of the elastic modulus of curaua fibers," *Matéria*, vol. 18, pp. 46–54, 2013.

[35] M. Maroufkhani, A. Katbab, W. Liu, and J. Zhang, "Polylactide (PLA) and acrylonitrile butadiene rubber (NBR) blends: the effect of ACN content on morphology, compatibility and mechanical properties," *Polymer*, vol. 115, pp. 37–44, 2017.

[36] S. BENSASON, J. MINICK, A. MOET et al., "Classification of Homogeneous Ethylene-Octene Copolymers Based on Comonomer content," *Journal of Polymer Science Part B: Polymer Physics*, vol. 34, pp. 1301–1315, 1996.

[37] J.-n. Yang and S.-b. Nie, "Effects of calcium sulfate whisker on the mechanical property, morphological structure and thermal degradation of poly (lactic acid) composites(lactic acid) composites," *Polymer Degradation and Stability*, vol. 144, pp. 270–280, 2017.